

Weak ferromagnetic spin and charge stripe order in $\text{La}_{5/3}\text{Sr}_{1/3}\text{NiO}_4$

R. Klingeler* and B. Büchner

Leibniz-Institute for Solid State and Materials Research IFW Dresden, 01171 Dresden, Germany

S-W. Cheong

Department of Physics and Astronomy, Rutgers University, Piscataway, New Jersey 08854

M. Hücker

Physics Department, Brookhaven National Laboratory, Upton, New York 11973

(Dated: November 9, 2018)

We present magnetisation and specific heat data of a $\text{La}_{5/3}\text{Sr}_{1/3}\text{NiO}_4$ single crystal in high magnetic fields. From the charge and spin stripe ordering temperatures, as well as a magnetic low temperature transition, we have constructed the electronic phase diagram for fields up to 14 Tesla. While the charge stripe ordering temperature T_{CO} is independent of the magnetic field, there is a significant shift of the spin stripe ordering temperature T_{SO} of about 1.5 K/Tesla, if the magnetic field is applied parallel to the NiO_2 -planes. The specific heat measurements indicate a large anomalous entropy change at T_{CO} . In contrast, no significant entropy change is observed at the spin stripe transition. The high field magnetisation experiments reveal the presence of in-plane weak ferromagnetic moments in the charge stripe ordered phase. From a phenomenological analysis, the magnetic correlation length of these moments is determined. We suggest that the weak ferromagnetism is due either to the presence of bond-centered charge stripes or to double exchange interactions across site-centered charge stripes.

PACS numbers:

I. INTRODUCTION

In cuprate, nickelate and manganite transition metal oxides the electronic ground state is determined by a complex interplay of charge and spin degrees of freedom. In some cases this interplay results in a nanoscopic modulation of the charge and spin density, which in the case of manganites seems to be closely connected to the colossal magnetoresistance. Other prominent examples are the stripe correlations in nickelates and cuprates. Here, the holes segregate into one dimensional charge stripes, thereby forming antiphase boundaries between spin stripes. In the cuprates the charge density modulation is weak and generally difficult to detect, in particular in superconducting cuprates where stripes are fluctuating.¹⁻³ In contrast, in the nickelates the stripe order is more pronounced, which makes its detection much easier.⁴⁻⁷ In recent years, stripe correlations in the nickelates have been studied with many different techniques, such as neutron scattering⁸⁻¹⁴, x-ray diffraction¹⁵⁻¹⁷, thermal conductivity¹⁸, NMR¹⁹⁻²¹, μSR ²², as well as optical²³ and Raman-spectroscopy^{24,25}. Nevertheless, very little is known about the thermodynamic properties of the stripe phase, such as the specific heat and the magnetisation in high magnetic fields. Thermodynamic methods were very successful in the investigation of the pseudo-cubic manganites, where spin and charge ordering phenomena are intimately connected and can be strongly influenced by an external magnetic field.²⁶⁻²⁹

In the layered nickelates the magnetism has strong two-dimensional (2D) character.^{9-11,30} In La_2NiO_4 the $S = 1$ spins of the Ni^{2+} ions form a 2D antiferromag-

netic (AFM) spin lattice with a weak interlayer coupling. Long range AFM spin order evolves at 330 K.³⁰ The substitution of La with Sr leads to a doping of the NiO_2 planes with hole charge carriers. Holes formally introduce Ni^{3+} -ions with $S = 1/2$ and cause the suppression of the conventional antiferromagnetic order. Charge and spin stripe order is observed over a wide range of hole doping ($0.135 \leq x \lesssim 0.7$).^{8,31} It is most pronounced at $x = 1/3$ and $x = 0.5$, where the stripe pattern is commensurate to the lattice.⁴ Stripes run diagonal to the Ni-O-Ni bonds. However, since in tetragonal symmetry ($I4/mmm$) there is no preferred stripe direction, one can find both, domains with stripes running parallel [110] as well as $[1\bar{1}0]$.⁴⁸ In spite of the intimate connection between charge and spin degrees of freedom, in nickelates charge stripes order at a significantly higher temperature than spin stripes ($T_{\text{SO}} < T_{\text{CO}}$).⁸ However, short range spin and charge stripe correlations are observed at temperatures significantly above T_{SO} and T_{CO} , respectively.^{9,15}

In this paper we present a study of the static magnetisation and the specific heat of a stripe ordered $\text{La}_{5/3}\text{Sr}_{1/3}\text{NiO}_4$ single crystal. Charge stripe order leads to pronounced anomalies in both specific heat and magnetisation. Measurements up to 14 T indicate that T_{CO} is independent of the magnetic field. In contrast, a strong field dependence is observed for T_{SO} if the magnetic field is applied parallel to the NiO_2 planes. While the spin stripe order is clearly detected in the magnetisation, a corresponding signature in the specific heat is not observed. Most interesting, in the charge stripe phase magnetisation curves show a weak ferromagnetic field depen-

dence. The analysis of our experimental results with simple phenomenological models provides estimates for the correlation length of the weak ferromagnetic moments. We discuss two different scenarios to explain our results. In particular, we suggest that the weak ferromagnetism is either due to the presence of bond-centered charge stripes or to double exchange interactions across site-centered charge stripes.

II. RESULTS AND DISCUSSION

A. Experimental

A large $\text{La}_{5/3}\text{Sr}_{1/3}\text{NiO}_4$ crystal was grown by the travelling-solvent floating-zone method.⁹ For the measurements, we cut and oriented a thin plate of $m = 74$ mg. The static magnetic susceptibility $\chi(T)$ with $\chi = M/B$ and the magnetisation $M(B)$ were measured with a vibrating sample magnetometer. An external field up to 14 T was applied parallel ($B \parallel ab$) as well as perpendicular ($B \perp ab$) to the NiO_2 planes. Corresponding data will be referred to as χ_{\parallel} , M_{\parallel} and χ_{\perp} , M_{\perp} , respectively. The specific heat c_p was measured for $B \parallel ab$ using a high resolution calorimeter. Here, we have applied two different quasi-adiabatic methods, continuous heating and heating pulses.^{29,32}

B. Magnetic susceptibility and specific heat

In order to identify the basic properties of $\text{La}_{5/3}\text{Sr}_{1/3}\text{NiO}_4$, we first show in Fig. 1 the susceptibility for $B = 1$ T applied parallel and perpendicular to the NiO_2 -planes. The magnetic field was applied well above T_{CO} before cooling the sample down to $T = 4.2$ K and taking the data with increasing temperature. Starting at high temperatures, one can see a small kink, which indicates the onset of the charge stripe order at $T_{\text{CO}} \approx 239$ K. At this kink the susceptibility shows a step-like decrease of similar size for both field directions (inset of Fig. 1). Below ~ 225 K the susceptibility increases monotonously and tends to saturate at low temperatures. The increase is particularly strong for χ_{\parallel} which stays always larger than χ_{\perp} . In addition to the well visible charge stripe order, there are two further transitions which do not lead to apparent anomalies in χ , but are clearly visible in the temperature derivative $\partial\chi_{\parallel}/\partial T$ in Fig. 1(b). Around $T_{\text{SO}} \sim 194$ K we observe a jump in $d\chi_{\parallel}/dT$ which expands between ~ 186 K and ~ 202 K. A comparison with neutron diffraction data shows that this anomaly marks the spin stripe ordering temperature. The second anomaly comprises of a minimum in $d\chi_{\parallel}/dT$ at $T_{\text{CA}} \sim 55$ K which marks the onset temperature for the canting of the spins in the magnetic stripes¹⁰ and the freezing of the moments in the charged domain walls^{33,34}. Note, that our present study gives evidence for a small canting even at $T > T_{\text{CA}}$

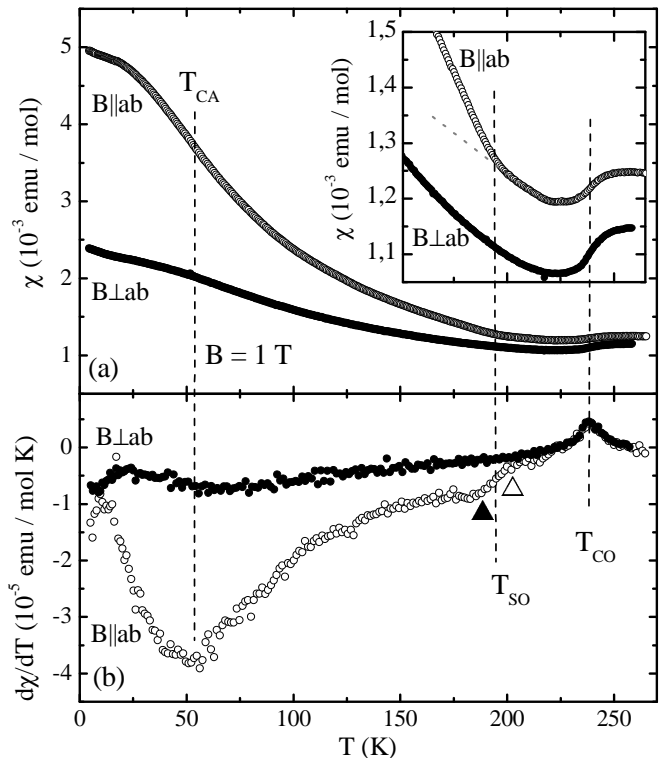


FIG. 1: (a) Static susceptibility $\chi = M/B$ of $\text{La}_{5/3}\text{Sr}_{1/3}\text{NiO}_4$ in a magnetic field of $B = 1$ T (FC) perpendicular and parallel to the ab -plane. The inset enlarges the temperature regime around T_{SO} and T_{CO} . The dotted line in the inset marks a linear extrapolation of χ_{\parallel} in order to highlight the changes at T_{SO} in the case of $B \parallel ab$. (b) Derivative of the static susceptibility. The charge stripe transition at T_{CO} (as confirmed from x-ray scattering³⁵), the spin stripe transition at T_{SO} (as confirmed from neutron diffraction^{9,10}), and the spin glass/spin reorientation transition at T_{CA} (cf. Ref. 10,14) are indicated by dashed lines.³³ The triangles show the temperature regime where a jump in $d\chi_{\parallel}/dT$ indicates the spin ordering.

which is different from the one discussed in Ref. 10 for $T < T_{\text{CA}}$.

The difference between χ_{\parallel} and χ_{\perp} at temperatures around T_{CO} can be explained with the anisotropy of the g -factor and the Van-Vleck susceptibility of the Ni-ions³⁶: $\Delta g \sim 0.08$ and $\Delta\chi_{\text{VV}} \approx 5 \times 10^{-5}$ emu/mol. Interestingly, the anisotropy does not change noticeably across T_{CO} . Below T_{SO} , however, it starts to increase significantly. We assume that the additional anisotropy at low temperatures is associated with the spin stripe order.

Fig. 2 (left scale) presents measurements of the specific heat for $B = 0$ and 14 T. Obviously, c_p is independent of the magnetic field within the experimental resolution. The onset of the charge stripe order at T_{CO} is indicated by a large anomaly in c_p , which follows from large entropy changes.³⁷ The jump-like shape of Δc_p evidences a second order phase transition. In contrast, no anomalous entropy changes are found at T_{SO} and T_{CA} , which is consistent with the absence of a pronounced anomaly

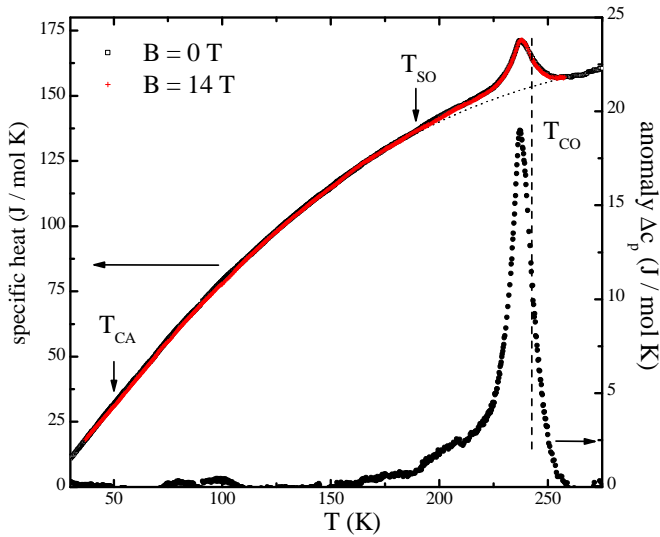


FIG. 2: (Colour online) Specific heat of $\text{La}_{5/3}\text{Sr}_{1/3}\text{NiO}_4$ for $B = 0$ (left ordinate). Applying $B = 14$ T does not change the results within the size of the data points. The dotted line refers to a polynomial function which has been fit to the data well outside the anomaly. Black circles (right ordinate) represent the difference of the data ($B = 0$) and the dotted line.

in the magnetic susceptibility. This result follows from the 2D nature of the magnetic correlations in the nickelates.^{9–11} Since strong 2D spin correlations develop already far above the 3D spin stripe ordering temperature, the transition at T_{SO} itself lacks a significant magnetic entropy change.

To estimate the anomalous entropy changes of the transition at T_{CO} , we have fit the mainly phononic contributions to $c_p(T)$ with a polynomial function well outside the region of the anomaly. Subtraction of this fit from $c_p(T)$ usually provides a reasonable lower limit for the total entropy changes. In our case the procedure yields $\Delta S_{\text{CO}} = \int \Delta c_p(T) dT \approx (2.0 \pm 0.3) \text{ J}/(\text{Mol} \cdot \text{K})$, i.e., $\Delta S_{\text{CO}} \approx (0.24 \pm 0.035) \cdot R$. The observed anomalous entropy changes are much smaller than $\Delta S_{\text{CO}} \approx 0.64 \cdot R$, which was estimated by applying a simple model for the complete charge ordering process.²⁶ This is not surprising since dynamic 2D short range charge correlations are present already at $T > T_{\text{CO}}$,^{9,15,16} which considerably reduces the entropy change at the 3D transition itself. In the limit of strong 2D correlations one even expects that anomalous entropy changes at T_{CO} due to charge degrees of freedom become negligible small.

In a recent theoretical study, in which the charge stripe disorder transition is considered to be driven by topological defects, it was indeed suggested that there are only minor changes of the charge stripe entropy at T_{CO} .^{38,39} This would imply that the experimentally observed entropy changes at T_{CO} are mainly due to spin degrees of freedom. A prominent example of such a scenario is the manganite $\text{La}_{7/8}\text{Sr}_{1/8}\text{MnO}_3$, where the entropy changes at the charge order transition can be attributed mainly to

the spin degrees of freedom.²⁹ In contrast to the manganites, the nickelates are characterized by a spin $S = 1$ state and a much weaker magneto-elastic coupling. Therefore, one might speculate that in the nickelates ΔS_{CO} is mainly due to charge degrees of freedom. Since in the nickelates the charge stripe order transition leads to an increase of the spin correlations, however, an additional contribution due to spin degrees of freedom is possible. From our experimental data it is not possible to distinguish whether spin or charge entropy accounts for the anomaly at T_{CO} .

The jump Δc_p at the phase transition can be evaluated quantitatively to estimate the magnetic field dependence of T_{CO} :

$$\frac{dT_{\text{CO}}}{dB} = -T_{\text{CO}} \frac{\Delta(\frac{\partial M}{\partial T})|_B}{\Delta c_{p,B}}. \quad (1)$$

From Fig. 1 and Fig. 2 we have determined the anomalies of the magnetisation and the specific heat to $\Delta(\partial M/\partial T) \approx (1.3 \pm 0.1) \times 10^{-6} \mu_B/(\text{Ni} \cdot \text{K})$ and $\Delta c_p \approx (20 \pm 1) \text{ J}/(\text{Mol} \cdot \text{K})$, respectively. With this values, Eqn. 1 yields $dT_{\text{CO}}/dB \approx -1 \times 10^{-4} \text{ K/T}$. Hence, the field dependence of T_{CO} is much too small to be detected experimentally, which is in agreement with the fact that we do not observe a field dependence in our data.

C. Electronic phase diagram

In Figure 3(a) we show χ of $\text{La}_{5/3}\text{Sr}_{1/3}\text{NiO}_4$ in different magnetic fields. For $B \perp ab$, the susceptibility is nearly independent of the magnetic field, except for minor changes in the spin glass/spin reorientation regime below T_{CA} . Thus, the magnetisation depends linearly on $B \perp ab$. In contrast, for $B \parallel ab$ a significant difference between the susceptibility at 1 T and 14 T is observed. As displayed in the inset of Fig. 3(a), this field dependence vanishes for $T > T_{\text{CO}}$, which means that for $B \parallel ab$ magnetisation curves are nonlinear only in the charge stripe ordered phase, and linear at higher temperatures (see Sec. IID). We will analyze this in more detail in the next section.

In Fig. 3(b), one can see that the temperature derivatives $\partial \chi_{\parallel}/\partial T$ at 5 T and 14 T exhibit the same three phase transitions at T_{CO} , T_{SO} and T_{CA} as for $B = 1$ T; there is a peak at T_{CO} , a jump at T_{SO} , and a minimum at T_{CA} . The data confirm that the charge stripe order temperature T_{CO} is independent of $B \leq 14$ T for both field directions. In contrast, for $B \parallel ab$ we find a clear shift of the spin stripe order temperature T_{SO} to higher temperatures and for T_{CA} a shift to lower temperatures. Note that due to the vicinity of T_{SO} and T_{CO} in high magnetic fields the upper limit of the jump at T_{SO} is hard to determine. In contrast, the lower limit (black triangle) at T_{SO}^* is always clearly visible. Therefore, we will use T_{SO}^* to discuss the field dependence of the spin stripe transition. For comparison, we will also extract T_{SO} as is illustrated

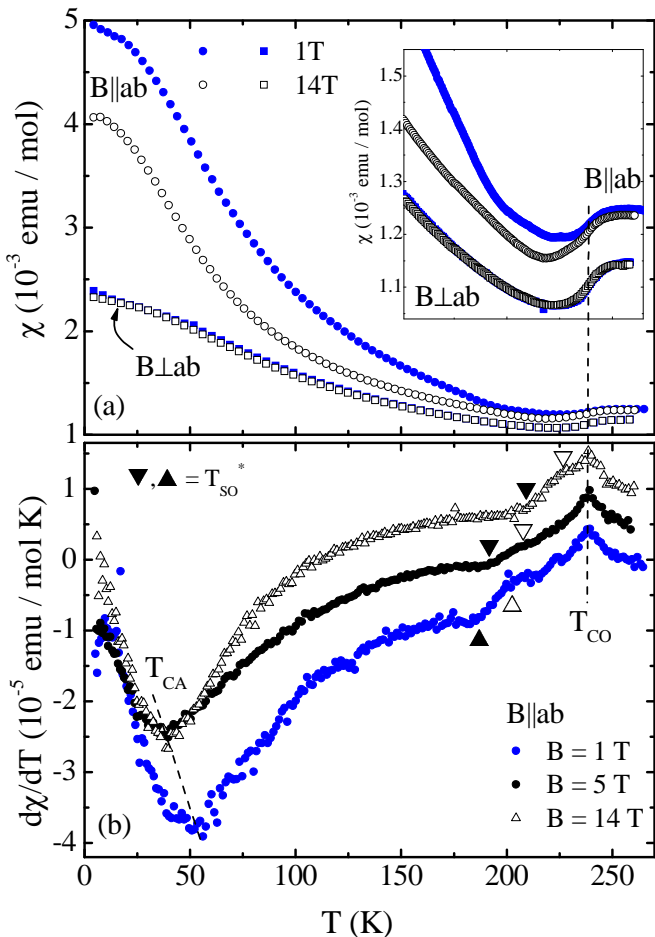


FIG. 3: (Colour online) (a) Static susceptibility χ of $\text{La}_{5/3}\text{Sr}_{1/3}\text{NiO}_4$ for $B = 1$ T (open symbols) and $B = 14$ T (FC) (full symbols) parallel and perpendicular to the ab -planes. The inset shows an enlargement of the temperature regime around T_{SO} and T_{CO} (only the y -axis is enlarged). (b) Derivative of χ_{\parallel} in magnetic fields $B = 1$ T, 5 T and 14 T parallel to the ab -planes. Data at $B = 5$ T and $B = 14$ T are shifted by 5×10^{-6} and 1×10^{-5} emu/(mol·K), respectively. Triangles mark the jump at T_{SO} (full triangle corresponds to T_{SO}^* , see text).

for $B = 1$ T in Fig. 1. From the signatures in $\partial\chi_{\parallel}/dT$ we have constructed the electronic phase diagram in Fig. 4. In detail, the field dependent study yields the following critical temperatures:

$B \parallel ab$ (T)	1	5	14
T_{SO}^* (K)	186 ± 2	191 ± 2	208 ± 2
T_{SO} (K)	194 ± 2	200 ± 6	218 ± 4
T_{CA} (K)	52 ± 3	40 ± 4	37 ± 4

Obviously, a magnetic field $B \parallel ab$ stabilizes the phase with long range ordered spin stripes. This is consistent with the fact that χ_{\parallel} in Fig. 1 and 1 increases below T_{SO} and tends to saturate below T_{CA} since the magnetic field always stabilizes the phase with the higher magnetisation. Extrapolating the phase boundary of $T_{\text{SO}}(B \parallel ab)$ to-

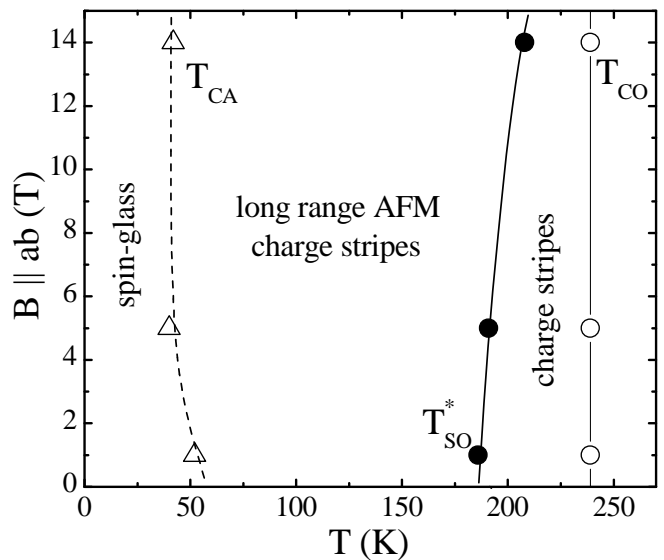


FIG. 4: Magnetic phase diagram of $\text{La}_{5/3}\text{Sr}_{1/3}\text{NiO}_4$ for a magnetic field $B \parallel ab$. T_{CO} , T_{SO}^* and T_{CA} mark the temperatures, where charge stripe order, long range spin stripe order and a spin reorientation occur, respectively. T_{CO} does also not change for $B \perp ab$.

wards higher fields suggests that $T_{\text{SO}}^* \approx T_{\text{CO}}$ for $B \parallel ab \approx (30 \pm 3)$ T. Therefore, magnetic fields higher than 30 T may also affect T_{CO} . Since for $B \perp ab$ corresponding anomalies at T_{SO} and T_{CA} are absent, no definite conclusion is possible for this field direction. However, the observation that around the spin stripe transition $dM_{\perp}/dT \sim 0$ might suggest that T_{SO} does not change significantly for this field direction (even though ΔS is also very small at T_{SO}).

D. Weak ferromagnetism below T_{CO}

The susceptibility data in Fig. 3(a) clearly indicate a nonlinear field dependence of the magnetisation at a constant temperature $T \lesssim T_{\text{CO}}$, when the magnetic field is applied parallel to the ab -plane. In order to study this phenomenon in more detail, we have measured $M(B)$ for $B \parallel ab$ by sweeping the field at different constant temperatures from $B = 0$ up to 14 T and then back to $B = 0$ (see Fig. 5).

As an example we show in Fig. 5 the $M(B)$ curves at $T = 100$ K. While for $B \perp ab$ the curve is perfectly linear, the one for $B \parallel ab$ shows a weak ferromagnetic type behaviour. The deviations from linearity become apparent when the field derivative of $M(B)$ is considered (see inset of Fig. 5). Nevertheless, also for $B \parallel ab$ the $M(B)$ curve is dominated by a linear contribution which may be attributed to the response of the antiferromagnetic ordered spins $S = 1$ in the magnetic stripes. In order to separate the nonlinear from the linear part, we have fit the high field behaviour in the field range $13 \text{ T} \leq B \leq$

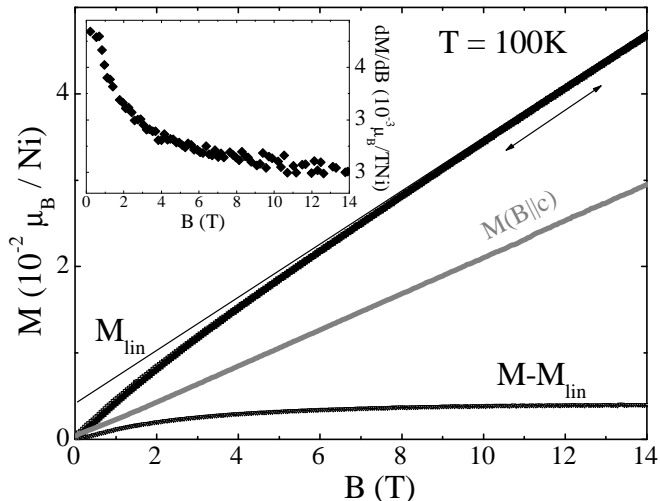


FIG. 5: Field dependence ($B \parallel ab$) of the magnetisation of $\text{La}_{5/3}\text{Sr}_{1/3}\text{NiO}_4$ at $T = 100$ K. The linear estimate M_{lin} highlights the slightly nonlinear field dependence of $M(B)$. Subtracting the linear part as extracted from $M(B \sim 13.5 \text{ T})$ results the nonlinear contribution. For comparison, M for $B \perp ab$ at $T = 100$ K is also plotted. The inset shows the field derivative of $M(B \parallel ab)$ which confirms the nonlinearity.

14 T with a linear function and subtracted the resulting straight line from the data. This procedure yields the $M - M_{\text{lin}}$ curves in Fig. 5, as well as in Fig. 6(b), which clearly show the weak ferromagnetic response. It is reasonable to assume, that there are magnetic moments in the ab -plane, which can be ferromagnetically aligned by a moderate magnetic field $B \parallel ab$. Interestingly, their saturation moment is of the order of several $10^{-3} \mu_B/\text{Ni}$, only, as can be seen in Fig. 5 and Fig. 6(b). To be able to align such a small moment at temperatures of the order of 100 K with a magnetic field of $B \sim 14$ T, these moments must be correlated over a large distance, i.e., the 2D magnetic correlation length in the NiO_2 planes must be large.

In Fig. 6 the $M(B)$ curves at various temperatures are plotted. Before going into detail, we mention that at low temperatures the magnetisation curves reveal a field hysteresis, which is particularly strong at 4 K [see Fig. 6(c)]. Therefore, we restrict the following quantitative analysis to temperatures $T > T_{\text{CA}}$, where the hysteresis is absent. The total magnetisation in Fig. 6(a) evidences a dominant linear and a small nonlinear magnetic contribution. As described above for $T = 100$ K, we have subtracted the linear part, which gives the weak ferromagnetic contribution $M - M_{\text{lin}}$ in Fig. 6(b) and (c). Obviously, the weak ferromagnetic contribution is present in the entire charge stripe ordered phase, but drastically decreases with increasing temperature, which is in perfect agreement with the field and temperature dependence of χ_{\parallel} in Fig. 3.

To obtain a better understanding of the weak ferromagnetic moments, we have analyzed the $M(B)$ curves

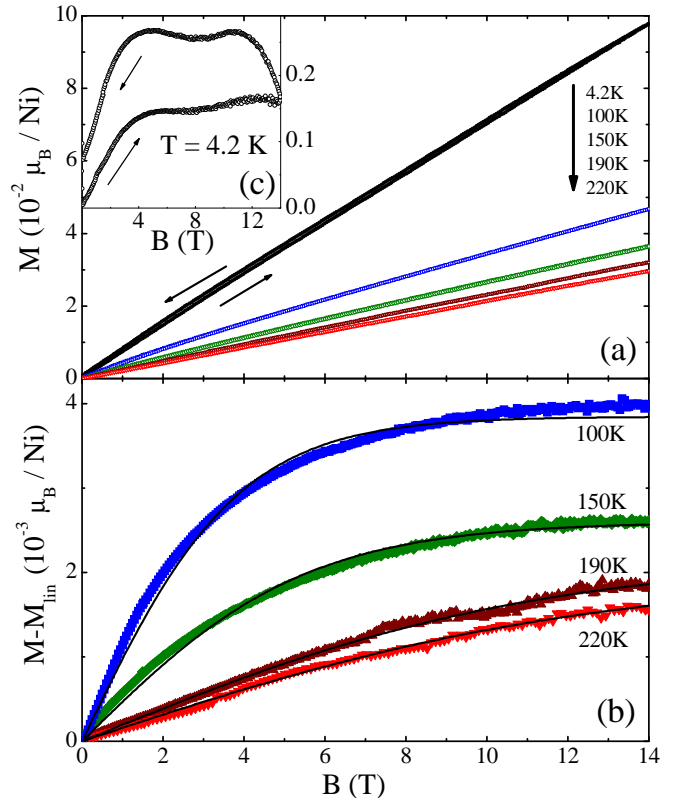


FIG. 6: (Colour online) (a) Field dependence ($B \parallel ab$) of the magnetisation of $\text{La}_{5/3}\text{Sr}_{1/3}\text{NiO}_4$ at various temperatures. (b)+(c) Nonlinear part of $M(B)$. The linear part has been extracted from $M(B \sim 13.5 \text{ T})$ at increasing field. At $T = 4.2$ K there is a field hysteresis. In the case of the $T = 4.2$ K data set we have subtracted the linear term found for increasing field from both parts of the magnetisation hysteresis. The straight lines in (b) are fits to the data according to Eqn. 2.

using a modified Brillouin function $B_{1/2}$:

$$M - B \left. \frac{\partial M}{\partial B} \right|_{\sim 13.5 \text{ T}} = M_S B_{\frac{1}{2}} \left(\frac{M_S \left(\frac{\xi_{2D}}{a} \right)^2 B_{\text{ext}}}{k_B T} \right) \quad (2)$$

$$= M_S \cdot \tanh \left(\frac{K B_{\text{ext}}}{T} \right) \quad (3)$$

where M_S is the saturation moment of the nonlinear contribution to $M(B)$, ξ_{2D} the 2D correlation length of small magnetic moments in the ab -plane, and a the in-plane lattice parameter. Hence, $(\xi_{2D}/a)^2$ is the number of 2D correlated moments. Equation 2 describes the continuous alignment of the moments in such a 2D correlated patch in an external field (cf. Ref. 40). The Brillouin function for $S = 1/2$ was chosen since we assume that, due to out-of-plane and in-plane spin anisotropies, the antiferromagnetic correlated patches have only two possible in-plane orientations. Fits according to Eqn. 2 were applied to the data in Fig. 6(b), with M_S and $K = M_S (\xi_{2D}/a)^2 / k_B$ being the variable parameters. The resulting curves are given by the solid lines in Fig. 6(b). Corresponding parameter values are listed in table I.

TABLE I: Magnetic field dependence ($B||ab$) of the magnetisation. Results of the analysis of $M(B)$ by using Eqn. 2.

$T(\text{K})$	$M_S(\mu_B/\text{Ni})$	$\xi_{2D}(\text{\AA})$	$\frac{\partial M}{\partial B} _{T,B\sim 13.5\text{ T}}(\frac{\mu_B}{\text{T Ni}})$
100	$3.6(\pm 1) \cdot 10^{-3}$	409(± 100)	$3.05 \cdot 10^{-3}$
150	$1.9(\pm 1) \cdot 10^{-3}$	580(± 100)	$2.4 \cdot 10^{-3}$
190	$2.1(\pm 1) \cdot 10^{-3}$	410(± 100)	$2.15 \cdot 10^{-3}$
220	$2.0(\pm 1) \cdot 10^{-3}$	437(± 100)	$2.0 \cdot 10^{-3}$

Obviously, the quantitative analysis provides a reliable description of the experimental data. We note, however, that for $T \geq 190\text{ K}$ the separation of linear and non-linear contributions to $M(T)$ is not unique because the magnetic field is not high enough. Therefore, at high temperatures the parameters in table I may exhibit a systematic uncertainty. In particular, we assume for all temperatures error bars of the order of $\sim 100\text{ \AA}$ for ξ_{2D} , and of the order of $1 \times 10^{-3} \mu_B/\text{Ni}$ for the magnetic moment M_S . Qualitatively, however, the nonlinear behaviour which is visible in the raw data clearly shows the presence of a weak ferromagnetic moment even at temperatures $T = 220\text{ K} > T_{\text{SO}}$.

Quantitatively, the analysis yields ξ_{2D} values, which are of the same order of magnitude for all temperatures. Before discussing a microscopic description of the weak ferromagnetism, we compare the values for ξ_{2D} provided by our macroscopic study with recent diffraction data. At least for low temperatures, our results are in a fair agreement with neutron diffraction results from Lee *et al.*, where no significant differences of the charge and the spin correlation lengths at $T = 100\text{ K}$ and $T = 150\text{ K}$ were found.⁹ Above the spin stripe order temperature, however, Lee *et al.* find significantly smaller values. In detail, their results on the in-plane correlation length perpendicular to the stripes are $\xi_{\perp}^C \approx 350\text{ \AA}$ for $T < T_{\text{SO}}$ and $\xi_{\perp}^C \approx 100\text{ \AA}$ for $T_{\text{SO}} < T < T_{\text{CO}}$.⁹ In recent hard x-ray studies of the charge stripe order, no significant changes of the correlation lengths was found between 20 K and 220 K.^{15,16} There is only a very small decrease of ξ^C upon cooling below T_{SO} .¹⁶ In particular, Du *et al.* find in-plane correlation lengths of $\xi_{\perp}^C \approx 185\text{ \AA}$ (perpendicular to the stripes) and $\xi_{\parallel}^C \approx 385\text{ \AA}$ (parallel to the stripes) for $T_{\text{SO}} < T \lesssim T_{\text{CO}}$.¹⁵ For lower temperatures, Ghazi *et al.* report $\xi_{\perp}^C \approx 165\text{ \AA}$ and $\xi_{\parallel}^C \approx 375\text{ \AA}$. Hence, despite the uncertainty of our analysis and the rough estimates, which are necessary to separate the linear and the nonlinear contributions to $M(B)$, the resulting ferromagnetic correlation lengths provided by our macroscopic study are in a fair agreement with the charge stripe correlation lengths of recent hard x-ray¹⁵⁻¹⁷ and neutron diffraction experiments⁹.

In summary, using measurements of the macroscopic magnetisation, we find weak ferromagnetic correlations with a correlation length, which is comparable to that

of the charge stripe correlations probed by diffraction techniques. In particular, the susceptibility measurements show that these weak ferromagnetic correlations exist in the whole charge stripe phase, which means that they persist also at temperatures above the spin stripe order transition. We note that, for temperatures $T_{\text{SO}} < T < T_{\text{CO}}$, 2D short range spin stripe correlations exist, but the correlation length of the spin stripe order is significantly reduced in this temperature regime. In contrast, the ferromagnetic correlation length provided by our macroscopic measurements does not change drastically at T_{SO} . We therefore assume that weak ferromagnetism must be intimately connected with the presence of charge stripes. In the following we discuss two different scenarios to explain our data. In particular, in Sec. II E we discuss possible evidence for bond-centered stripes and present in Sec. II F a microscopic charge and spin stripe model, which is consistent with the presence of weak ferromagnetic moments.

E. Site- versus bond-centered stripes

A priori, there are different possible sources for the weak ferromagnetic moments, because there are two magnetic subsystems in the charge stripe phase: (i) the spins $S = 1/2$ in the charge stripes, and (ii) the spins $S = 1$ in the magnetic stripes. From nuclear magnetic resonance measurements it was inferred that the spins in the charge stripes are nearly free for $T > T_{\text{CA}}$.³⁴ In contrast, a recent inelastic neutron scattering study evidences for dynamic quasi-1D antiferromagnetic correlations among the charge stripe electrons with a correlation length of $\sim 15\text{ \AA}$.⁴¹ For both scenarios, the magnetic response of the charge stripe moments is not expected to exhibit a weak ferromagnetic moment within the ab -planes. Therefore, we believe that the weak ferromagnetism is not solely connected to the spins of the charge stripes, but has to be linked to the spin stripe correlations, as well.⁴²

A key question which arises in this context concerns the position of the charge stripes with respect to the lattice. In the most simple sketch of the stripe phase, the charge stripes reside only on the Ni-sites. The doped holes, however, are mainly O: $2p$ -like.⁴³ In general, the domain walls might be either centered on the rows of Ni ions (site-centered stripes) or on the rows of oxygens (bond-centered stripes).⁴⁴ This is illustrated in Fig. 7. (This figure is similar to Fig. 1 in Ref. 44.)

In the case of site centered charge stripes the magnetic domains are two spins wide [see Fig. 7(a)]. All spins in the magnetic stripes are equivalent. Spins are aligned antiferromagnetically within the magnetic domains as well as across the charge stripes. Consequently, all spins are compensated. For bond-centered stripes the effective width of the magnetic domains amounts to three spins (cf. Fig. 7(b)). In this case, 1/3 of the spins of a spin stripe remain uncompensated. Furthermore, the coupling between nearest neighbour spins across a charge

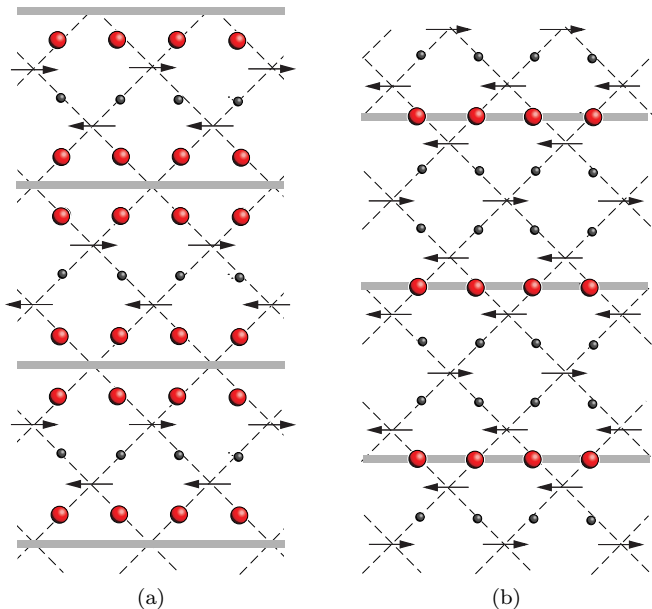


FIG. 7: (Colour online) Site- and bond-centered stripes. Dashed lines show the underlying square lattice. Ni^{2+} -spins in spin stripes are indicated by arrows, oxygen sites by circles. Large (red) circles indicate high hole density. Grey bars show domain walls. Canting of Ni-spins with respect to the stripe direction is neglected. (a) Site-centered domain walls. All Ni moments are equivalent and compensated. (b) Bond-centered domain walls. Ni moments near domain walls and in the center of spin stripes, respectively, are inequivalent. A net magnetic moment is possible. The figure is similar to Fig. 1 in Ref. 44.

stripe is ferromagnetic. For this ferrimagnet type spin structure a perfect compensation of the spins is not expected and a net magnetic moment might appear. It is worth mentioning that in the bond-centered case the spins in the center of the spin stripes and the ones near the charged domain walls are not equivalent.

Recent diffraction and transmission-electron microscopy data on doped nickelates suggest the presence of both bond-centered and site-centered stripes.^{44–46} Thus, a net magnetic moment might indeed arise from the fact that at least some of the charge stripes are bond-centered. In this scenario, the observed value M_S of the saturation magnetisation of the weak ferromagnetic moments (cf. table I) is directly connected to the amount of bond-centered stripes below T_{CO} .⁴⁷ However, a quantitative comparison with our data is not possible since neither the net moment of a bond-centered stripe nor the ratio of a potential mixing of site- and bond-centered stripes is known.

Qualitatively, however, the presence of bond-centered domain walls might account for our observation of weak ferromagnetism in the charge stripe phase. In this scenario our observation of weak ferromagnetism nicely agrees with the observation of bond-centered stripes in doped nickelates (cf. Ref. 44–46). In the next para-

graphs we show, however, that our experimental results can also be explained by a scenario based on the presence of site-centered stripes.

F. Phenomenological model of weak ferromagnetic stripes

If one assumes a charge stripe order with site-centered stripes [cf. Fig. 7(a)], the weak ferromagnetic moments are only very small perturbations of the antiferromagnetic spin order. In the following we consider the case that this weak ferromagnetic perturbation results from a small canting of the antiferromagnetic ordered Ni^{2+} -spins. In particular, we propose a microscopic model where the antiferromagnetic coupling of the Ni^{2+} spins in the spin stripes via the Ni^{3+} ions in the charge stripes is superposed by a weak canting. The saturation magnetisation at low temperatures is of the order of $M_S \approx 4 \times 10^{-3} \mu_B/\text{Ni}$ [see Fig. 6(b)]. This value of M_S corresponds to an average canting angle of the Ni-spins in the spin stripes of the order of $\phi \lesssim 0.1^\circ$. We mention, that this deviation from the perfect antiferromagnetic spin structure is too small to be detected by neutron diffraction experiments.

Fig. 8(a) sketches one charge stripe and the adjacent (canted) Ni^{2+} spins. The grey arrows show the perfect antiferromagnetic arrangement of the spins, based on recent experiments with polarized neutrons.¹⁰ In this arrangement, spins are canted $\sim 40^\circ$ ($T > T_{\text{CA}}$) from the stripe direction and coupled antiferromagnetically across the stripes. Our results imply an additional non-collinear canting of the spins by an angle ϕ as indicated by the black arrows in Fig. 8(a). Note that the canting ϕ is strongly exaggerated for visibility. Since the canting direction for all spins bordering a particular charge stripe is the same, it leads to a weak ferromagnetic moment spatially centered on the charge stripe. It is worth mentioning that due to the canting charge stripes are no longer perfect antiphase boundaries of the underlying antiferromagnetic spin order, although the antiferromagnetic coupling across the charge stripe is still by far the dominating energy scale.

Figure 8(b) presents the zero field arrangement of two stripes. For the sake of simplicity, we first limit the discussion to the long range spin stripe ordered phase for $T_{\text{CA}} < T < T_{\text{SO}}$. Furthermore, we assume that the correlations along the c -axis can be neglected for the discussion of the in-plane spin correlations. As sketched in Fig. 8(b), the spin canting in adjacent stripes competes with the antiferromagnetic superexchange J between nearest neighbour Ni^{2+} spins within the spin stripes, and the interstripe coupling J' across the charge stripes. A recent inelastic neutron study suggests $J = 15 \pm 1.5$ meV and $J' = 7.5 \pm 1.5$ meV.⁴⁸ In contrast, a theoretical analysis³⁹ based on similar neutron data⁴⁹ suggests $J' \approx 0.9J$, i.e. the coupling across the charge stripes is not much smaller than the coupling between nearest neighbours within the

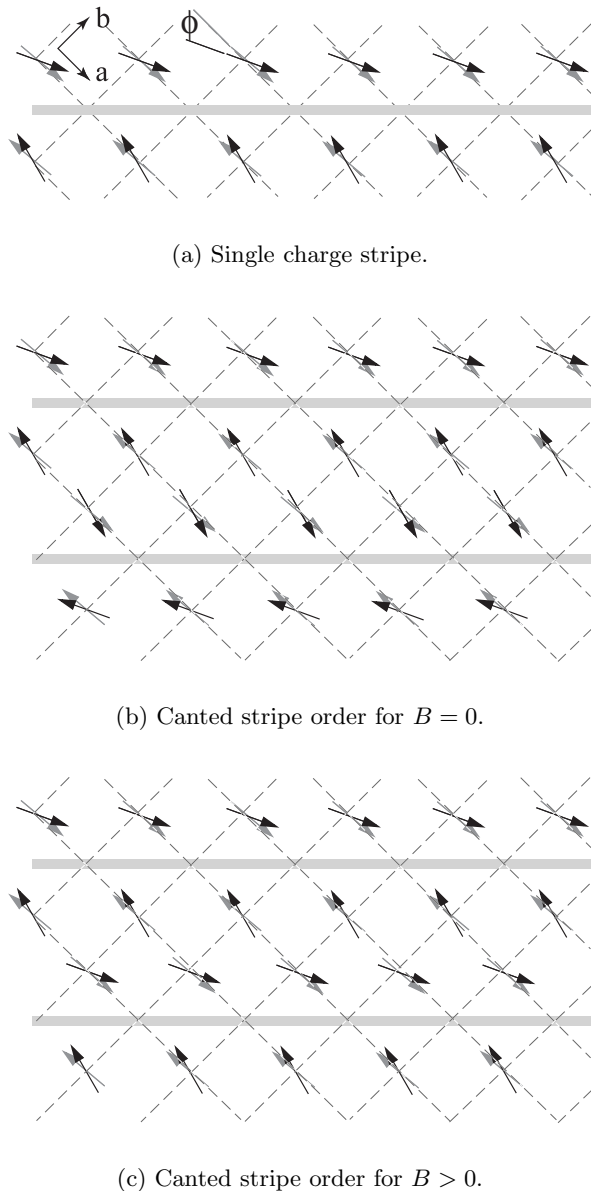


FIG. 8: Schematic picture of the spin arrangement (black arrows) in the magnetic stripes of $\text{La}_{5/3}\text{Sr}_{1/3}\text{NiO}_4$, where the Ni^{2+} -Spins are canted with respect to the perfect antiferromagnetic order (grey arrows) due to ferromagnetic interactions. Arrows represent Ni^{2+} ($S = 1$), Ni^{3+} and oxygen sites are neglected for clarity. (a) Charge stripe with a resulting weak ferromagnetic moment due to a small canting angle ϕ . (b) Canted spin and charge stripe order in zero magnetic field with alternating weak ferromagnetic moments in adjacent stripes and (c) for $B > 0$ with a macroscopic weak ferromagnetic moment.

spin stripes. However, both studies imply that, due to the large value of J , in zero magnetic field the weak ferromagnetic moments of adjacent charge stripes are aligned antiferromagnetically (cf. Fig. 8(b)).

According to our experimental data, the weak ferromagnetic moments become ferromagnetically aligned in

a large external magnetic field. At an intermediate temperature of 100 K a field of the order of 10 T is sufficient to align most of the moments. The resulting spin arrangement is presented in Fig. 8(c). As one can see, this process lifts the perfect antiferromagnetic arrangement of the spins within a spin stripe. A rough estimate, however, shows that a weak spin canting against the dominating antiferromagnetic coupling is indeed favorable. The gain of Zeeman energy due to the ferromagnetic alignment competes with the loss of superexchange energy due to the canting of nearest neighbour Ni spins. In fact, the alignment of the small magnetic moments results in a gain of Zeeman energy of the order of $\Delta M \cdot B \sim 2.6 \times 10^5$ erg/mol. On the other hand, adjacent spin stripe moments are canted by $2\phi \lesssim 0.2^\circ$, which leads to a loss of superexchange energy of the order $JN_A/3(1 - \cos(2\phi)) \sim 3 \times 10^4$ erg/mol. This rough estimate shows that, for a sufficiently high magnetic field, the loss of superexchange energy due to the canting is overcompensated by the gain of Zeeman energy.

We mention that Fig. 8 contains strong simplifications. Since in $\text{La}_{5/3}\text{Sr}_{1/3}\text{NiO}_4$ the out-of-plane anisotropy ($K_c = (0.07 \pm 0.01)$ meV) is significantly smaller than in La_2NiO_4 ^{30,48}, the even smaller in-plane anisotropy should be negligible for our experiment. Therefore, for a magnetic field of several Tesla applied along any in-plane direction, the Ni^{2+} spins should always be oriented nearly perpendicular to the field.⁵⁰

G. Microscopic mechanism

In the following we may speculate about the underlying mechanism that causes the weak ferromagnetism in the case of site-centered stripes. One possible candidate is the Dzyaloshinskii-Moriya (DM) interaction. A precondition for this interaction is the lack of inversion symmetry with respect to the center of the involved ions. An excellent example for the DM exchange interaction is La_2CuO_4 , where the inversion symmetry of the Cu-O-Cu bond is broken due to the tilting of the CuO_6 octahedra. In the stripe phase of $\text{La}_{5/3}\text{Sr}_{1/3}\text{NiO}_4$, deviations from the perfect tetragonal symmetry were detected.⁵ However, corresponding lattice distortions, associated with modulations of the Ni-O bond length, are not supposed to lift the inversion symmetry. Therefore, we believe that the DM interaction is irrelevant in the stripe phase of $\text{La}_{5/3}\text{Sr}_{1/3}\text{NiO}_4$.

Instead, we suggest another source for the weak ferromagnetism: A magnetic exchange which causes ferromagnetic interactions between ions of different valency is provided by the double exchange (DE) mechanism. DE is most prominent in the doped manganites and describes at least qualitatively the CMR effect.^{51,52} Other mixed valency compounds with both ferromagnetism and metallic-like conductivity, which are discussed in terms of double exchange, are CrO_2 ⁵³ and Fe_3O_4 ⁵⁴. In contrast, in the doped nickelates it

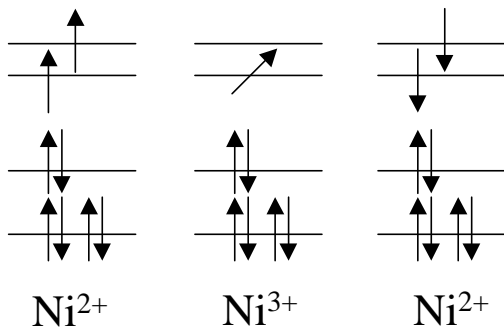


FIG. 9: Schematic drawing of a $\text{Ni}^{2+}\text{-Ni}^{3+}\text{-Ni}^{2+}$ configuration. In addition to the antiferromagnetic coupling between the Ni^{2+} ions the double exchange mechanism may infer a ferromagnetic interaction.

is quite unusual to refer to DE. However, since an individual Ni^{3+} ion (i.e. a hole in a charge stripe) is surrounded by four Ni^{2+} ions, one might speculate whether DE causes the weak ferromagnetism. As is sketched in Fig. 9, where the configuration of one Ni^{3+} and two adjacent Ni^{2+} is displayed, the DE mechanism provides a maximum gain of the kinetic energy of the e_g -electrons if the Ni^{2+} -spins are parallel. However, DE competes with the antiferromagnetic coupling of the Ni^{2+} -spins, which is the dominating magnetic exchange. Therefore, the central Ni^{3+} -spins are frustrated. The DE can only account for a small weak ferromagnetic moment, which is in agreement with the experiment. Note, that in this microscopic model the Ni^{3+} e_g -spins are supposed to be slightly polarized, too. However, it remains to be checked with local techniques, whether or not the spins in the charge stripes contribute to the weak ferromagnetism. We also note, that DE is not restricted to the charge ordered phase. Due to the fact that spin and charge correlations rapidly decrease above T_{CO} , however, the magnetic correlation length ξ_{2D} (cf. Eq. 2) becomes very small, too. Therefore, a linear field dependence of the magnetisation of the weak

ferromagnetic moments is expected above T_{CO} .

III. CONCLUSION

In summary, we have presented measurements of the magnetisation and the specific heat of a $\text{La}_{5/3}\text{Sr}_{1/3}\text{NiO}_4$ single crystal in high magnetic fields. We have shown that the onset of charge stripe order is connected with large entropy changes. These entropy changes are independent of magnetic fields $B \leq 14$ T. In contrast, the onset of the long range spin order does not result in a noticeable anomaly of the specific heat. In the susceptibility, we find characteristic features at T_{CO} and T_{SO} which allow to determine the electronic phase diagram. While the charge stripe order temperature T_{CO} is independent of the magnetic field, there is a pronounced field dependence of T_{SO} . We also find a weak ferromagnetic moment which occurs in the entire charge stripe ordered phase. Analyzing the field dependence of the magnetisation provides the weak ferromagnetic correlation length which is similar to the charge stripe correlation length. Two different scenarios to explain our results were discussed. We suggest that the weak ferromagnetism is due either to the presence of bond-centered charge stripes or to double exchange interactions across site-centered charge stripes.

Acknowledgments

We thank J. Zaanen and C. Hess for stimulating discussions, J. Geck for experimental advise, and M. Rümeli for critical reading of the manuscript. R.K. acknowledges support by the DFG through KL 1824/1-1. The work of M.H. at Brookhaven was supported by the Office of Science, US Department of Energy under Contract No. DE-AC02-98CH10886.

* r.klingeler@ifw-dresden.de; Present address: Laboratoire National des Champs Magnétiques Pulsés, 31432 Toulouse, France.

¹ J. Zaanen, cond-mat/0103255

² J.M. Tranquada, B.J. Sternlieb, J.D. Axe, Y. Nakamura, S. Uchida, Nature **375**, 561 (1995)

³ K. Yamada, C.H. Lee, K. Kurahashi, J. Wada, S. Wakimoto, S. Ueki, H. Kimura, Y. Endoh, S. Hosoya, G. Shirane, R.J. Birgeneau, M. Greven, M.A. Kastner and Y. J. Kim, Phys. Rev. B **57**, 6165 (1998)

⁴ S.-W. Cheong, H.Y. Hwang, C.H. Chen, B. Batlogg, L.W. Rupp, and S.A. Carter, Phys. Rev. B **49**, R7088 (1994)

⁵ J.M. Tranquada, D.J. Buttrey, V. Sachan, and J. E. Lorenzo, Phys. Rev. Lett. **73**, 1003 (1994)

⁶ B.J. Sternlieb, J.P. Hill, U.C. Wildgruber, G.M. Luke, B.

Nachumi, Y. Moritomo and Y. Tokura, Phys. Rev. Lett. **76**, 2169 (1996)

⁷ C.H. Chen, S.-W. Cheong, and A.S. Cooper, Phys. Rev. Lett. **71**, 2461 (1993)

⁸ H. Yoshizawa, T. Kakeshita, R. Kajimoto, T. Tanabe, T. Katsufuji, and Y. Tokura, Phys. Rev. B **61**, R854 (2000)

⁹ S.-H. Lee and S.-W. Cheong, Phys. Rev. Lett. **79**, 2514 (1997)

¹⁰ S.-H. Lee, S.-W. Cheong, K. Yamada, and C.F. Majkrzak, Phys. Rev. B **63**, 060405(R) (2001)

¹¹ R. Kajimoto, T. Kakeshita, H. Yoshizawa, T. Tanabe, T. Katsufuji, and Y. Tokura, Phys. Rev. B **64**, 144432 (2001)

¹² P.G. Freeman, A.T. Boothroyd, D. Prabhakaran, D. González, and M. Enderle Phys. Rev. B **66**, 212405 (2002)

¹³ R. Kajimoto, K. Ishizaka, H. Yoshizawa, and Y. Tokura,

- Phys. Rev. B **67**, 014511 (2003)
- ¹⁴ P.G. Freeman, A.T. Boothroyd, D. Prabhakaran, M. Enderle, and C. Niedermayer, Phys. Rev. B **70**, 024413 (2004)
- ¹⁵ C-H. Du, M.E. Ghazi, Y. Su, I. Pape, P.D. Hatton, S.D. Brown, W.G. Stirling, M.J. Cooper, and S-W. Cheong, Phys. Rev. Lett. **84**, 3911 (2000)
- ¹⁶ M.E. Ghazi, P.D. Spencer, S.B. Wilkins, P.D. Hatton, D. Mannix, D. Prabhakaran, A.T. Boothroyd, S.-W. Cheong, Phys. Rev. B **70**, 144507 (2004)
- ¹⁷ K. Ishizaka, T. Arima, Y. Murakami, R. Kajimoto, H. Yoshizawa, N. Nagaosa, Y. Tokura, Phys. Rev. Lett. **92**, 196404 (2004)
- ¹⁸ C. Hess, B. Büchner, M. Hücker, R. Gross, and S-W. Cheong, Phys. Rev. B **59**, R10397 (1999)
- ¹⁹ Y. Yoshinari, P.C. Hammel and S-W. Cheong, Phys. Rev. Lett. **82**, 3536 (1999)
- ²⁰ I.M. Abu-Shiekh, O.O. Bernal, A.A. Menovsky, H.B. Brom, and J. Zaanen, Phys. Rev. Lett. **83**, 3309 (1999)
- ²¹ I.M. Abu-Shiekh, O. Bakharev, H.B. Brom, and J. Zaanen, Phys. Rev. Lett. **87**, 237201 (2001)
- ²² T. Jestaedt, K.H. Chow, S.J. Blundell, W. Hayes, F.L. Pratt, B.W. Lovett, M.A. Green, J.E. Millburn, and M.J. Rosseinsky, Phys. Rev. B **59**, 3775 (1999)
- ²³ T. Katsufuji, T. Tanabe, T. Ishikawa, Y. Fukuda, T. Arima, and Y. Tokura, Phys. Rev. B **54**, R14230 (1996)
- ²⁴ G. Blumberg, M. V. Klein, and S-W. Cheong, Phys. Rev. Lett. **80**, 564 (2000)
- ²⁵ K. Yamamoto, T. Katsufuji, T. Tanabe, and Y. Tokura, Phys. Rev. Lett. **80**, 1493 (1998)
- ²⁶ A.P. Ramirez, P.L. Gammel, S-W. Cheong, D.J. Bishop, P. Chandra, Phys. Rev. Lett. **76**, 447 (1996)
- ²⁷ J.E. Gordon, R.A. Fisher, Y.X. Jia, N.E. Phillips, S.F. Reklis, D.A. Wright and A. Zettl, Phys. Rev. B **59**, 127 (1999)
- ²⁸ S. Uhlenbruck, R. Teipen, R. Klingeler, B. Büchner, O. Friedt, M. Hücker, H. Kierspel, T. Niemöller, L. Pinsard, A. Revcolevschi and R. Gross, Phys. Rev. Lett. **82**, 185 (1999)
- ²⁹ R. Klingeler, J. Geck, R. Gross, L. Pinsard-Gaudart, A. Revcolevschi, S. Uhlenbruck, and B. Büchner, Phys. Rev. B **65**, 174404 (2002)
- ³⁰ K. Nakajima, K. Yamada, S. Hosoya, Y. Endoh, M. Greven, and R.J. Birgeneau, Z. Phys. B **96**, 479 (1995)
- ³¹ V. Sachan, D.J. Buttrey, J.M. Tranquada, J.E. Lorenzo, and G. Shirane, Phys. Rev. B **51**, 12742 (1995).
- ³² H. Kierspel, H. Winkelmann, T. Auweiler, W. Schlabitz, B. Büchner, V.H.M. Duijn, N.T. Hien, A.A. Menovsky, and J.J.M. Franse, Physica C **262**, 177 (1996)
- ³³ The labeling of the phase transitions follows Ref. 10.
- ³⁴ I.M. Abu-Shiekh, O.O. Bernal, H.B. Brom, M.L. de Kok, A.A. Menovsky, J.T. Witteveen, and J. Zaanen, cond-mat/9805124
- ³⁵ We confirmed the onset of the charge stripe order by verifying the corresponding superstructure reflection (1.33,1.33,3) with hard x-ray diffraction. T. Niemoeller, J. Geck and C. Hess, unpublished data.
- ³⁶ A. Abragam and B. Bleaney, Electron Paramagnetic Resonance of Transition Metal Oxides, New York 1986
- ³⁷ We mention that our measurements on single crystalline $\text{La}_{5/3}\text{Sr}_{1/3}\text{NiO}_4$ rule out anomalous entropy changes due to a further phase transition at $T \sim 264\text{K}$ ($> T_{\text{CO}}$) which have been found in previous measurements of the specific heat on a polycrystalline sample by Ramirez *et al.* (Ref. 26).
- ³⁸ F. Krüger and S. Scheidl, Phys. Rev. Lett. **89**, 095701 (2002)
- ³⁹ F. Krüger and S. Scheidl, Phys. Rev. B **67**, 134512 (2003)
- ⁴⁰ M. Hücker, H.-H. Klauss, and B. Büchner, Phys. Rev. B **70**, 220507(R) (2004)
- ⁴¹ A.T. Boothroyd, P.G. Freeman, D. Prabhakaran, A. Hiess, M. Enderle, J. Kulda, F. Altorfer, Phys. Rev. Lett. **91**, 257201 (2003)
- ⁴² As already stated, short range antiferromagnetic correlations are present far above T_{SO} .
- ⁴³ H. Eisaki, S. Uchida, T. Mizokawa, H. Namatame, A. Fujimori, J. van Elp, P. Kuiper, G.A. Sawatzky, S. Hosoya, H. Katayama-Yoshida, Phys. Rev. B **45**, 12513 (1992)
- ⁴⁴ J.M. Tranquada, P. Wochner, A.R. Moodenbaugh, D.J. Buttrey, Phys. Rev. B **55**, R6113 (1997)
- ⁴⁵ P. Wochner, J.M. Tranquada, D.J. Buttrey, V. Sachan, Phys. Rev. B **57**, 1066 (1998)
- ⁴⁶ Jianqi Li, Yimei Zhu, J.M. Tranquada, K. Yamada, D.J. Buttrey, Phys. Rev. B **67**, 012404 (2003)
- ⁴⁷ Note that the experimental error for M_S in table I is significant.
- ⁴⁸ A.T. Boothroyd, D. Prabhakaran, P.G. Freeman, S.J.S. Lister, M. Enderle, A. Hiess, and J. Kulda, Phys. Rev. B **67**, 100407(R) (2003)
- ⁴⁹ P. Bourges, Y. Sidis, M. Braden, K. Nakajima, and J.M. Tranquada, Phys. Rev. Lett. **90**, 147202 (2003)
- ⁵⁰ Even in La_2NiO_4 the in-plane anisotropy amounts to $|J_X| - |J_Y| \approx 3.5 \times 10^{-3} J$, only. For $\text{La}_{5/3}\text{Sr}_{1/3}\text{NiO}_4$, we assume a spin-flop field of the order of 10^{-1} T. Due to the twinning, the spin-flop feature is probably smeared out.
- ⁵¹ C. Zener, Phys. Rev. **82**, 403 (1951)
- ⁵² P.W. Anderson and H. Hasegawa, Phys. Rev. **100**, 675 (1955)
- ⁵³ M.A. Korotin, V.I. Anisimov, D.I. Khomskii, and G.A. Sawatzky, Phys. Rev. Lett. **80**, 4305 (1998)
- ⁵⁴ P.A. Cox, Transition Metal Oxides. An Introduction to their Electronic Structure and Properties, Oxford University Press (1992)